JVI Journals.ASM.org

The Histone Deacetylase Inhibitor Valproic Acid Lessens NK Cell Action against Oncolytic Virus-Infected Glioblastoma Cells by Inhibition of STAT5/T-BET Signaling and Generation of Gamma Interferon

Christopher A. Alvarez-Breckenridge,[a,b] Jianhua Yu,[c] Richard Price,[a,b] Min Wei,[d] Yan Wang,[b] Michal O. Nowicki,[b] Yoonhee P. Ha,[d] Stephen Bergin,[a] Christine Hwang,[d] Soledad A. Fernandez,[d,e] Balveen Kaur,[b,d] Michael A. Caligiuri,[d] and E. Antonio Chiocca[b,d]

Medical Scientist Training Program,[a] Dardinger Laboratory for Neuro-oncology and Neurosciences, Department of Neurological Surgery,[b] Division of Hematology,[c] The Ohio State University Comprehensive Cancer Center,[d] and Center for Biostatistics,[e] The Ohio State University Medical Center and The James Cancer Hospital and Solove Research Institute, Columbus, Ohio, USA

Tumor virotherapy has been and continues to be used in clinical trials. One barrier to effective viral oncolysis, consisting of the interferon (IFN) response induced by viral infection, is inhibited by valproic acid (VPA) and other histone deacetylase inhibitors (HDACi). Innate immune cell recruitment and activation have been shown to be deleterious to the efficacy of oncolytic herpes simplex virus (oHSV) infection, and in this report we demonstrate that VPA limits this deleterious response. VPA, administered prior to oHSV inoculation in an orthotopic glioblastoma mouse model, resulted in a decline in NK and macrophage recruitment into tumor-bearing brains at 6 and 24 h post-oHSV infection. Interestingly, there was a robust rebound of recruitment of these cells at 72 h post-oHSV infection. The observed initial decline in immune cell recruitment was accompanied by a reduction in their activation status. VPA was also found to have a profound immunosuppressive effect on human NK cells *in vitro*. NK cytotoxicity was abrogated following exposure to VPA, consistent with downmodulation of cytotoxic gene expression of granzyme B and perforin at the mRNA and protein levels. In addition, suppression of gamma IFN (IFN-γ) production by VPA was associated with decreased STAT5 phosphorylation and dampened T-BET expression. Despite VPA-mediated immune suppression, mice were not at significantly increased risk for HSV encephalitis. These findings indicate that one of the avenues by which VPA enhances oHSV efficacy is through initial suppression of immune cell recruitment and inhibition of inflammatory cell pathways within NK cells.

Despite intense investigations to improve the standard of therapy for glioblastoma (GBM), current regimens result in approximately 15 months of median survival following initial diagnosis, emphasizing the need for new therapies. Oncolytic viruses (OV) are promising biological agents, intensely investigated for nearly 2 decades. These naturally occurring and biologically engineered viruses, which are designed to replicate in a relatively selective manner within tumors and culminate in the destruction of the host's cancer cells (1, 10), have demonstrated effectiveness in preclinical models. Five different clinical trials have tested oncolytic herpes simplex virus (oHSV) (22, 35, 36, 47, 50), and a maximum tolerated dose was not achieved and toxicity was not demonstrated. Additionally, oncolytic adenovirus (11), Newcastle disease virus (16), and reovirus (14) have been shown to be safe in dose escalation trials in humans with malignant glioma; moreover, there are ongoing clinical trials with measles virus (24), retrovirus (45), parvovirus H-1, poliovirus, and Seneca Valley virus (see http://www.clinicaltrials.gov/ct2/results?term=glioblastoma+AND+virus). However, therapeutic efficacy has been elusive to demonstrate. It is evident that efficacy should depend on the ability of the initially injected oHSV to replicate and distribute within the GBM mass. Identification of both barriers in the host that could limit cytotoxic viral replication against the tumor and possible cotherapies that could overcome such barriers would be a fertile ground of research to improve tumor virotherapy efficacy.

Based on the work from our laboratory and others, the initial phases of the innate immune response are likely to have a deleterious impact on virotherapy, by limiting effective biodistribution. In particular, the activated response of both NK cells and microglia-macrophages to oncolytic HSV (oHSV) infection impedes viral infection, replication, and ultimate tumor lysis (17, 18). For instance, clodronate-mediated depletion of peripheral phagocytic cells resulted in a 5-fold increase in oHSV titers in intracranial glioblastoma. Other approaches have been used to circumvent the barrier of innate immunity, including the use of tumor-trafficking immune cells (2, 54), second-generation oncolytic viruses expressing immunoevasive proteins (4), and pharmacologic adjuvants that suppress the antiviral immune response (5, 17, 25, 26, 28, 31, 46, 56).

In another similar approach, we have demonstrated that pharmacological modulation of the innate immune response by administration of cyclophosphamide (CPA) prior to oHSV treat-

Received 28 June 2011 **Accepted** 14 January 2012
Published ahead of print 8 February 2012
Address correspondence to E. Antonio Chiocca, EA.Chiocca@osumc.edu, or Michael Caligiuri, michael.caligiuri@osumc.edu.
C. A. Alvarez-Breckenridge and J. Yu contributed equally to this article.
Supplemental material for this article may be found at http://jvi.asm.org/.

doi:10.1128/JVI.05545-11

ment resulted in enhanced OV efficacy as measured by viral replication and overall animal survival (25, 28). We proceeded to evaluate gamma interferon (IFN-γ) production 72 h after a rodent model of glioma was treated with oHSV and showed that protein levels of IFN-γ were robustly increased following oHSV administration. However, CPA pretreatment was able to attenuate this response (17). Additionally, treatment with 4-hydroxyperoxy-CPA (4HC), the intermediate active metabolite of CPA, impaired monokine-induced IFN-γ production by NK cells (17). Taken together, these findings demonstrate that pharmacological modulation of innate immunity in the context of oHSV therapy, as seen with CPA, improves therapeutic efficacy.

In addition to CPA, valproic acid (VPA) has been used by both our laboratory and others to enhance oHSV therapy (33, 41, 46). VPA is a commonly used, FDA-approved, antiepileptic agent with histone deacetylase inhibitory functions. VPA and other histone deacetylase inhibitors (HDACi) have been found to possess anticancer activity on their own (15, 29, 37). Moreover, HDACi have been shown to upregulate the transcriptional activity of virally delivered transgenes both *in vitro* and *in vivo* (9, 13, 59) and to prevent the transcriptional activation of IFN-stimulated genes (ISGs) in response to IFN treatment and viral infection (7, 20, 43, 53). These features make HDACi an attractive cotherapy to augment HSV-based oncolytic virotherapy. Our laboratory has previously demonstrated that pretreatment with VPA can upregulate the transcriptional activity of HSV genes, limit the antiviral effects of IFN by inhibiting the induction of ISGs, and enhance the *in vivo* therapeutic efficacy of oHSV therapy (46).

To date, an examination of the ability of VPA to modulate the innate immune response to oHSV infection has been lacking. Based on our previous findings that inhibition of immune recruitment enhances oHSV efficacy (17) and that VPA synergizes with oHSV therapy by suppressing the virus-mediated type I IFN response (46), we hypothesized that VPA also enhances oHSV therapy efficacy by altering the kinetics of immune cell recruitment, activation, and inflammation. Here we report both the cellular immune response to oHSV-infected glioblastoma in the presence of VPA and the ability of VPA to suppress NK cell-mediated inflammation. Our findings suggest that VPA imparts a transient immunosuppressive environment following oHSV infection. Moreover, VPA attenuates NK cell-mediated cytotoxicity against oHSV-infected tumors and IFN-γ production with concomitant STAT5/T-BET inhibition. Since VPA is currently being evaluated as an antineoplasm agent and as cotherapy for OV infections, these findings uncover important functional properties of VPA for both fields.

MATERIALS AND METHODS

Cell culture. The glioblastoma cells used included human glioblastoma cell lines (U87dEGFR, U251, and Gli36dEGFR) and primary human glioblastoma cells enriched for stem-like cell properties by passage in animal flanks (X12, but originally named GBM12) (21). These cells were cultured in Dulbecco's modified Eagle's medium (DMEM; Invitrogen, Carlsbad, CA) supplemented with 10% fetal bovine serum, penicillin (100 U/ml), and streptomycin (100 μg/ml). Human astrocytes (ScienCell, San Diego, CA) were cultured in astrocyte medium supplemented with 2% fetal bovine serum (FBS). Donor derived-NK cells and the NK-92 cell line were cultured in RPMI-1640 (Invitrogen, Carlsbad, CA) supplemented with 10% fetal bovine serum, penicillin (100 U/ml), and streptomycin (100 μg/ml). Interleukin-2 (IL-2) (150 U/ml) was included in the media to maintain cultured NK-92 cells. Cells were cultured at 37°C in media supplemented with 5% CO_2.

Animal studies. Athymic mice (Charles River Laboratories, Wilmington, MA) were anesthetized by intraperitoneal administration of ketamine (100 mg/kg of body weight) and xylazine (20 mg/kg) and stereotactically injected with 1×10^5 human U87dEGFR glioblastoma cells into the right frontal lobe of the brain (2 mm lateral and 1 mm anterior to bregma at a depth of 3 mm). For VPA (Sigma-Aldrich, St. Louis, MO) administration, drug was administered intraperitoneally (300 mg/kg) two times at 12-h intervals. The following day, mice were injected intratumorally with oHSV (46). For CPA (Bristol-Myers Squibb Co., Princeton, NJ) administration, drug was administered intraperitoneally (300 mg/kg) 24 h prior to viral injection (28). The U87dEGFR cells were allowed to grow for 9 days, and animals were subsequently randomly divided into groups that were injected intratumorally either with rQNestin34.5, an oncolytic HSV-1 genetically modified to replicate specifically in glioblastoma cells (27), in 3 μl of Hanks' balanced salt solution (HBSS) or with vehicle. For experiments with wild-type (WT) HSV1 (F strain), 10^3 or 10^4 PFU of virus was inoculated into the right frontal lobe of glioblastoma-free athymic mice.

Flow cytometric analysis. Mononuclear cells were isolated from oHSV-infected brains by the use of a previously described procedure with minor modifications (38). In brief, 6, 24, or 72 h after infection, mice were sacrificed, brain tissue was harvested, and the tumor-bearing hemispheres were placed in DMEM. The tissue was homogenized through a 70-μm-pore-size strainer. Single-cell preparations were resuspended in 30% Percoll (GE Healthcare, Uppsala, Sweden), overlaid on 70% Percoll, and centrifuged at 1,300 × *g* for 30 min at 4°C. Cells at the 70% to 30% interface were collected and washed with phosphate-buffered saline (PBS). Cells isolated from the brain were treated with Fc Block (BD, San Jose, CA). Cells were then stained with anti-mouse immune cell surface markers for 30 min at 4°C. The following anti-mouse antibodies were used: CD3-fluorescein isothiocyanate (CD3-FITC), DX5-phycoerythrin (DX5-PE), CD3-peridinin chlorophyll protein (CD3-PerCP), CD62L-allophycocyanin (CD62L-APC), and CD11b-PE (BD); CD62L-FITC, CD69-FITC, Ly49d-APC, NKp46-FITC, CD11b-PerCP, CD3-APC, and CD45-APC (eBioscience, San Diego, CA); Ly-6c-FITC (Biolegend); and DX5-APC (Miltenyi Biotec, Auburn, CA). Following antibody staining, cells were resuspended in 1% formalin and analyzed using a FACSCalibur (Becton Dickinson, Mountain View, CA).

Quantitative real-time reverse transcriptase (RT) PCR. Total RNA from tumor-bearing hemispheres or enriched human NK cells was isolated using an RNeasy lipid tissue Midikit or RNeasy Minikit, respectively (Qiagen, Valencia, CA). A total of 5 μg of total RNA was reverse transcribed using random hexamers and a SuperScript first-strand cDNA synthesis system (Invitrogen). Quantitative real-time PCR was done with cDNA samples diluted 1:100 in water and performed using SYBR green PCR Master Mix and an ABI Prism 7500 sequence detection system (Applied Biosystems, Foster City, CA). Murine primers were IFN-γ and GAPDH (glyceraldehyde-3-phosphate dehydrogenase) internal control. Human primers were IFN-γ, perforin (PRF1), granzyme B (GRZB), STAT5a, STAT5b, and 18S. Primer and probe sequences are available upon request. We also used a Mouse Inflammatory Cytokines & Receptors RT^2 Profiler PCR array (Super Array Bioscience Corporation, Frederick, MD), according to the manufacturer's instructions, to evaluate changes in the expression of genes encoding 84 mouse cytokines and their receptors in brain tumor tissue in response to valproic acid treatment with oncolytic virus relative to oncolytic virus treatment alone. The array includes controls to assess cDNA quality and DNA contamination.

STAT5 shRNA knockdown. To knock down STAT5 expression in NK-92 cells, a short hairpin RNA (shRNA) approach was undertaken. The designed shRNA oligonucleotides (sequences are available upon request) were annealed and ligated into a pSIH-H1–green fluorescent protein (pSIH-H1–GFP) lentiviral vector (System Biosciences, Mountain View, CA) to make a STAT5-shRNA construct. The STAT5-shRNA lentiviral

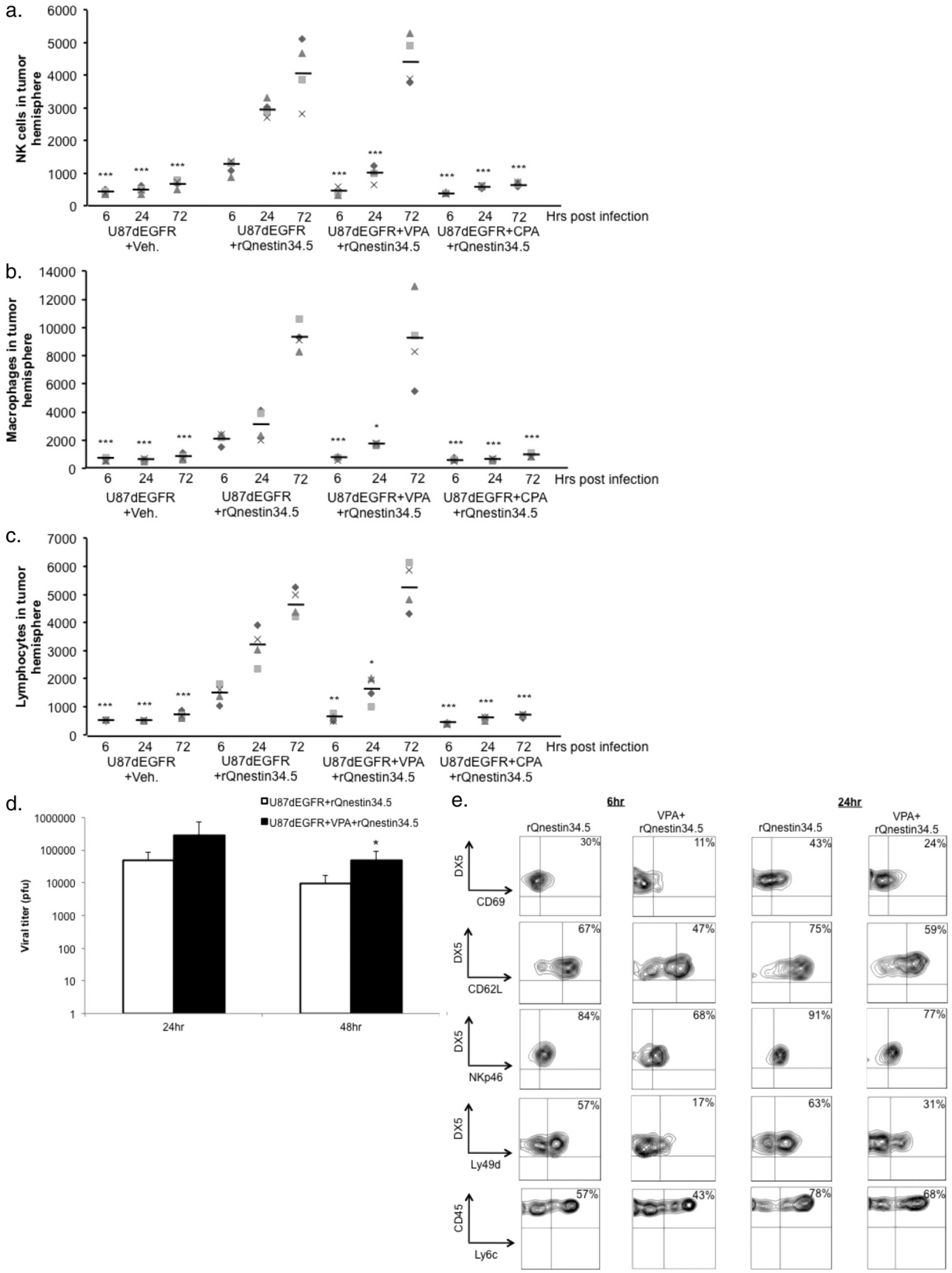

FIG 1 Valproic acid suppresses immune cell infiltration following oHSV administration. (a) Human U87dEGFR cells (10^5) were implanted intracranially into athymic mice brains ($n = 3$ to 6/group) and allowed to grow for 9 days. rQNestin34.5 (10^4 PFU/3 μl of vehicle) or vehicle was then stereotactically inoculated, using the same coordinates. For VPA-treated mice, two VPA treatments were performed at 12-h intervals the day before oHSV inoculation. For CPA-treated mice, CPA was administered 48 h before oHSV inoculation. Tumor-bearing hemispheres were harvested 72 h later to quantify the total number of NK cells by

construct and its empty control vector were transfected into 293T cells. The viruses were harvested, used to infect NK-92 cells, and then washed three times with RPMI 1640 medium. These were used to infect NK-92 cells, followed by three washes with RPMI-1640 media. Infected NK-92 cells were expanded and maintained in the RPMI media containing 20% FBS and IL-2 as aforementioned. Cells positive for GFP and/or expressing STAT5 shRNA were enriched by cell sorting using a BD FACSArial II cell sorter.

Viral titration. To measure viral replication, we followed the procedures outlined by Otsuki et al. (46). Briefly, mice bearing U87dEGFR gliomas were treated with saline solution or VPA and rQNestin34.5 (10^4 PFU) before sacrifice at the 24 or 48 h time point. The tumor-bearing hemispheres were placed in DMEM and sonicated on ice. Cellular debris was pelleted by centrifugation, brain lysates were subsequently plated on Vero cells, and plaques were quantified.

NK cell isolation. NK cells were enriched from peripheral blood leukopacks of healthy donors (American Red Cross, Columbus, OH) by the use of RosetteSep cocktail (StemCell Technologies, Vancouver, Canada). The enriched NK cells were then further purified using positive-selection CD56 magnetic bead sorting (Miltenyi Biotec). Once NK cells were isolated, they were cultured overnight in 10% RPMI media prior to being used in downstream applications.

Cytotoxicity assay. The panel of human glioblastoma cells was plated overnight at 10^4 cells/well. Where noted, cells were treated with 5 mM VPA for 14 h prior to infection, washed, and then infected with rQNestin34.5 (46). Cells were infected for 8 h with rQNestin34.5 (multiplicity of infection [MOI] of 1.0) or mock infected. Human NK cells were added at an effector/target ratio of 12.5:1 in the presence of human IL-15 (Miltenyi Biotec) (10 ng/ml). The coculture growth was allowed to proceed for 4 h at 37°C. Glioblastoma lysis was assessed by measuring glucose 6-phosphate dehydrogenase released from lysed cells by the use of a Vybrant cytotoxicity assay kit (Molecular Probes, Eugene, OR) (19).

ELISA. Purified human NK cells (see NK cell isolation procedure above) were cultured overnight *in vitro* in the presence or absence of 5 mM VPA. Additionally, NK cells were either left untreated or stimulated overnight with various cytokines (IL-12, IL-15, or IL-18 [each at 10 ng/ml]) or Toll-like receptor stimulants, lipopolysaccharide (LPS) (1 μg/ml) and Pam2CSK4 (100 μg/ml). Supernatants were collected for detection of IFN-γ by enzyme-linked immunosorbent assay (ELISA) as previously described (60). The remaining cells were collected and processed for quantitative real-time reverse transcriptase PCR as described above. IL-12 was kindly provided by Genetics Institute Inc. (Cambridge, MA), and IL-15 was kindly provided by Amgen. IL-18 was purchased from R & D Systems, LPS from Sigma-Aldrich, and Pam2CSK4 from InvivoGen (San Diego, CA). To evaluate levels of IFN-γ in tumor-bearing brains, treated with or without rQNestin34.5 and with VPA or HBSS, the right cerebral hemisphere was homogenized in an 8 M urea solution containing 0.2 M NaCl and 0.1 M Tris base for protein extraction, followed by IFN-γ ELISA as previously described (60).

Western blotting. To assess protein levels or activities of STAT5, T-BET, perforin (PRF1), and granzyme B (GRZB), direct cell lysates or total protein extractions were prepared from enriched human NK cells treated overnight in the absence or presence of various amounts of VPA or cytokine stimulants. Western blotting was performed as previously described (60). Assessment of the protein level of actin by Western blotting was included to control for protein loading. Antibodies used for Western blotting were the mouse monoclonal antibody (MAb) T-BET (Santa Cruz), the mouse MAb perforin (Abcam, Cambridge, MA), and the rabbit MAb phospho-STAT5^{Tyr694} and rabbit MAb granzyme B (Cell Signaling, Danvers, MA).

Statistical analyses. Total NK was log transformed to achieve normality. A generalized linear model was used to study the interaction effect (calculated as group × time). Pairwise comparisons of treatments versus rQNestin34.5 infection within time periods were performed and *P* values adjusted using Tukey's method. For each cell type, a generalized linear model was used to study the interaction effect calculated as group × time for percent cell population determinations. Pairwise comparisons within time periods were also adjusted using Tukey's method. Two-sample *t* tests with Bonferroni adjustments were used to compare fold differences in expression levels and percent glioblastoma lysis. Log-rank tests were used to compare survival curves.

RESULTS

Valproic acid suppresses immune cell infiltration following oHSV administration. We first confirmed the nature of the immune cell infiltration after intracranially administering rQNestin34.5 into an orthotopic human glioblastoma (U87dEGFR) xenograft. At 6, 24, and 72 h postinfection, fluorescence-activated cell sorter (FACS) analysis was used to quantify the presence of NK cells (DX5$^+$ CD3$^-$), macrophages (CD45^{high} CD11b$^+$), and lymphocytes (CD45^{high} CD11b$^{low/-}$) in the tumor-bearing hemispheres of these mice. Compared to mice treated with vehicle, there was a robustly significant time-dependent increase in the numbers of recruited NK cells (Fig. 1a), macrophages (Fig. 1b), and lymphocytes (Fig. 1c) in tumor-bearing brain hemispheres. Valproic acid has been shown to enhance OV efficacy through inhibition of type I interferon and its downstream pathways (46) and degradation of cyclin D1 and vascular endothelial growth factor (VEGF) inhibition (33) and to increase mitochondrial depolymerization and caspase 3/9 cleavage (41). When VPA was administered prior to oHSV injection, we detected a significant decrease in the recruitment of NK cells, macrophages, and lymphocytes within the brain 6 and 24 h after infection. By 72 h after infection, the VPA effect was abrogated, with innate cell recruitment rebounding to baseline levels (Fig. 1a to c). No significant change in immune cell infiltration was observed in tumor-bearing mice infected with vehicle in the presence or absence of VPA (see Fig. S1 in the supplemental material). Prior to oHSV administration, we treated mice with cyclophosphamide, a panimmunosuppressant that has been demonstrated by multiple groups to enhance oHSV efficacy

FACS analysis. (b and c) Athymic mice were implanted with tumor, treated with VPA or CPA, and inoculated with rQNestin34.5 as described for panel a. rQNestin34.5 (10^4 PFU/3 μl) or vehicle was then inoculated at the site of tumor implantation, and mice were sacrificed at different time points in order to quantify by FACS analysis the number of macrophages (CD45^{high} CD11b$^+$) (b) and lymphocytes (CD45^{high} CD11b$^{low/-}$) (c) in tumor-bearing hemispheres following treatment. Individual events are plotted for each condition and time point tested. Horizontal bars indicate the mean values for individual events. Pairwise comparisons to U87dEGFR plus rQNestin34.5 within each time point and a generalized linear model to study interaction effects were performed. *P* values were adjusted using Tukey's method. (d) Athymic mice were implanted with tumor, treated with VPA or HBSS, and inoculated with rQNestin34.5 (10^4 PFU/3 μl) at the site of tumor implantation as described for panel a. After 24 or 48 h, mice were sacrificed, tumor-bearing hemispheres were sonicated, and brain lysates were plated on Vero cells for quantification of viral plaques. *P* values were calculated using Student's *t* test. (e) Athymic mice were implanted with tumor, treated with VPA or HBSS, and inoculated with rQNestin34.5 (10^4 PFU/3 μl) at the site of tumor implantation as described for panel a. After 6 or 24 h, mice were sacrificed and tumor-bearing hemispheres were processed so that the NK cells or macrophages could be analyzed using FACS analysis. Each panel consists of a representative dotplot demonstrating the altered surface expression of NK cells expressing NK cell activation markers (CD69, CD62L, NKp46, and Ly49d) and a macrophage activation marker (Ly49c) following viral administration. Fluctuations in the *x-y* intersection for each panel are based on the relative intensity of staining for each tested marker. Table S1 in the supplemental material provides averages and ranges that summarize the total number of experiments. *, $P < 0.05$; **, $P < 0.01$; ***, $P < 0.001$. Error bars represent ± standard deviations.

through its immunomodulatory properties (17, 32, 34, 40, 49). Similar to previous work from our laboratory (17), CPA robustly attenuated the recruitment of NK cells, macrophages, and lymphocytes within the tumor-bearing hemisphere (Fig. 1a to c). However, the magnitude and time course of this suppression were different from those observed with VPA, suggesting that these two drugs impart different profiles of immune cell kinetics to the site of infection. These findings suggest that, in addition to its ability to modulate intracellular antiviral mechanisms within the infected tumor, VPA initially attenuates the kinetics and abundance of recruited antiviral mediators after oHSV infection.

oHSV inoculation with VPA reduces the inflammatory response. In our previous study (46), we had shown increased oHSV titers in brain tumors of mice that had been cotreated with VPA and oHSV. This increase in oHSV titers was measured 72 h after infection, and yet the data in Fig. 1a to c show that the VPA effect on NK cells and macrophages had already dissipated by this time point. Therefore, to determine if the VPA-mediated reduction of numbers of NK cells and macrophages observed before 72 h also led to increased oHSV replication at those time points, we assayed oHSV titers in gliomas at 24 and 48 h after VPA and oHSV cotherapy. Figure 1d shows that, indeed, there was a significant increase in oHSV levels in tumors explanted from mice cotreated with VPA and oHSV versus control and oHSV at the 48 h time point. At the 24 h time point, a trend toward increased titers was also observed. This temporally associates VPA's reduction of NK and macrophage cell infiltration with increased *in vivo* oHSV replication.

Since VPA attenuated the recruitment of NK cells and macrophages at early time points after oHSV infection, we became interested in evaluating the phenotypic features of these cells, particularly the early activation marker CD69 (39), the lymphocyte homing antigen CD62L (8), the natural cytotoxicity receptor NKp46 (57), and the activating receptor Ly49d (52), on NK cells and the Ly-6c activation marker on macrophages. We found that oHSV administration induced a unique phenotype for these markers on immune cells recruited to the site of infection. However, when VPA was coadministered with oHSV, there was a decrease at 6 and 24 h postinfection in surface expression of these activation markers on NK cells (Fig. 1e). Additionally, macrophage staining of Ly-6c was reduced with VPA cotherapy (Fig. 1e). No significant change in the expression of these activation markers were seen in tumor-bearing mice treated with a virus injection control in the presence or absence of VPA (see Table S1b in the supplemental material). Collectively, these findings demonstrate that VPA not only suppresses the recruitment of these immune mediators but also attenuates their activation in response to oncolytic viral infection. In order to evaluate the consequences of these changes, a mouse inflammatory array was used to examine the changes in inflammatory gene expression imparted by VPA cotherapy, either 24 or 72 h after oHSV infection. Consistent with the recruitment and phenotyping FACS data, VPA suppressed oHSV-induced inflammation 24 h postinfection (Fig. 2a; see also Table S2a in the supplemental material) but had no effect 72 h postinfection (Fig. 2b; see also Table S2b in the supplemental material). Finally, we also found that at 24 h postinfection, VPA suppressed IFN-γ gene (Fig. 2c) and protein (Fig. 2d) expression following oHSV inoculation. However, there was no change at 72 h postinfection and VPA exposure did not alter the basal level of IFN-γ production in vehicle-treated mice (data not shown).

VPA suppression of IFN-γ production is associated with STAT5/T-BET inhibition. To extend these *in vivo* findings, we used human NK cells to investigate the ability of VPA treatment to suppress their cytotoxicity *in vitro*. NK cells are primed for IFN-γ production following exposure to IL-12 and IL-15 or IL-18 (58). We confirmed this by evaluating IFN-γ transcripts following overnight cultures of NK cells from human donors in the presence of IL-12 plus IL-15 or IL-12 plus IL-18 (Fig. 3a). However, when VPA was added to the overnight culture, IFN-γ gene expression was significantly decreased. This suppression was also observed at the protein level. VPA abrogated secreted IFN-γ production both in the NK-92 cell line (Fig. 3b) and across three separate human donors (Fig. 3c). In a control experiment, we also were able to show that VPA did not affect the viability of NK cells (data not shown). Moreover, we found that VPA treatment inhibited monokine-stimulated IFN-γ production and that this was associated with attenuation of STAT5 phosphorylation and T-BET expression, a master regulator of IFN-γ gene expression (48, 55, 60) (Fig. 3d). In addition, we tried to determine whether VPA inhibited NK cell activation with noncytokine stimuli mediated through Toll-like receptors. Interestingly, we found that IFN-γ production by NK cells in response to LPS (TLR4 stimulus) and Pam2CSK4 (TLR2 and TLR4 stimulus) was either very low or undetectable by ELISA (see Fig. S2 in the supplemental material).

To further provide mechanistic evidence for the role played by STAT5 in VPA's effect on NK cells, we utilized shRNA-mediated reduction of STAT5 (STAT5a and STAT5b) expression in NK-92 cells (Fig. 3e). There was significantly less inhibition by VPA of IFN-γ production in STAT5 shRNA-expressing NK cells exposed to cytokine stimuli than in control shRNA NK cells (58.4% IFN-γ production inhibition versus 40.0%; $P < 0.05$). Taken together, these data strongly suggest that VPA reduced the ability of cytokine-stimulated NK cells to generate IFN-γ, that this was associated with reduced levels of phosphorylated STAT-5 and T-BET in NK cells, and that knockdown of STAT-5 transcript reduced VPA's inhibition of NK cell activation.

Mediators of NK cell cytotoxicity are reduced by VPA. In addition to IFN-γ production, NK cell activation is also associated with cell-mediated cytotoxicity. In order to test the role of VPA in this process, we analyzed transcripts of perforin and granzyme B following overnight growth in culture with increasing amounts of VPA across samples from three donors. VPA mediated a significant dose-dependent attenuation in gene expression of these two mediators of NK cell cytotoxicity (Fig. 4a). The observed dose-dependent reduction in levels of perforin and granzyme B transcripts also correlated with a decrease in protein levels (Fig. 4b), although VPA inhibited granzyme A and Fas ligand production at the transcript level but not the protein level (data not shown). Overall, these findings reveal that VPA potently suppresses mechanisms of both NK cell-mediated cytotoxicity and cytokine production.

NK cell-mediated killing of oHSV-infected glioblastoma cells is suppressed by VPA. Because VPA potently suppressed NK cell activation, we tested its ability to suppress NK cell-mediated killing of oHSV-infected glioblastoma cells. IL-15-activated human NK cells readily killed Gli36dEGFR, U87dEGFR, and U251 glioblastoma cells and X12 "stem-like" glioblastomas that were

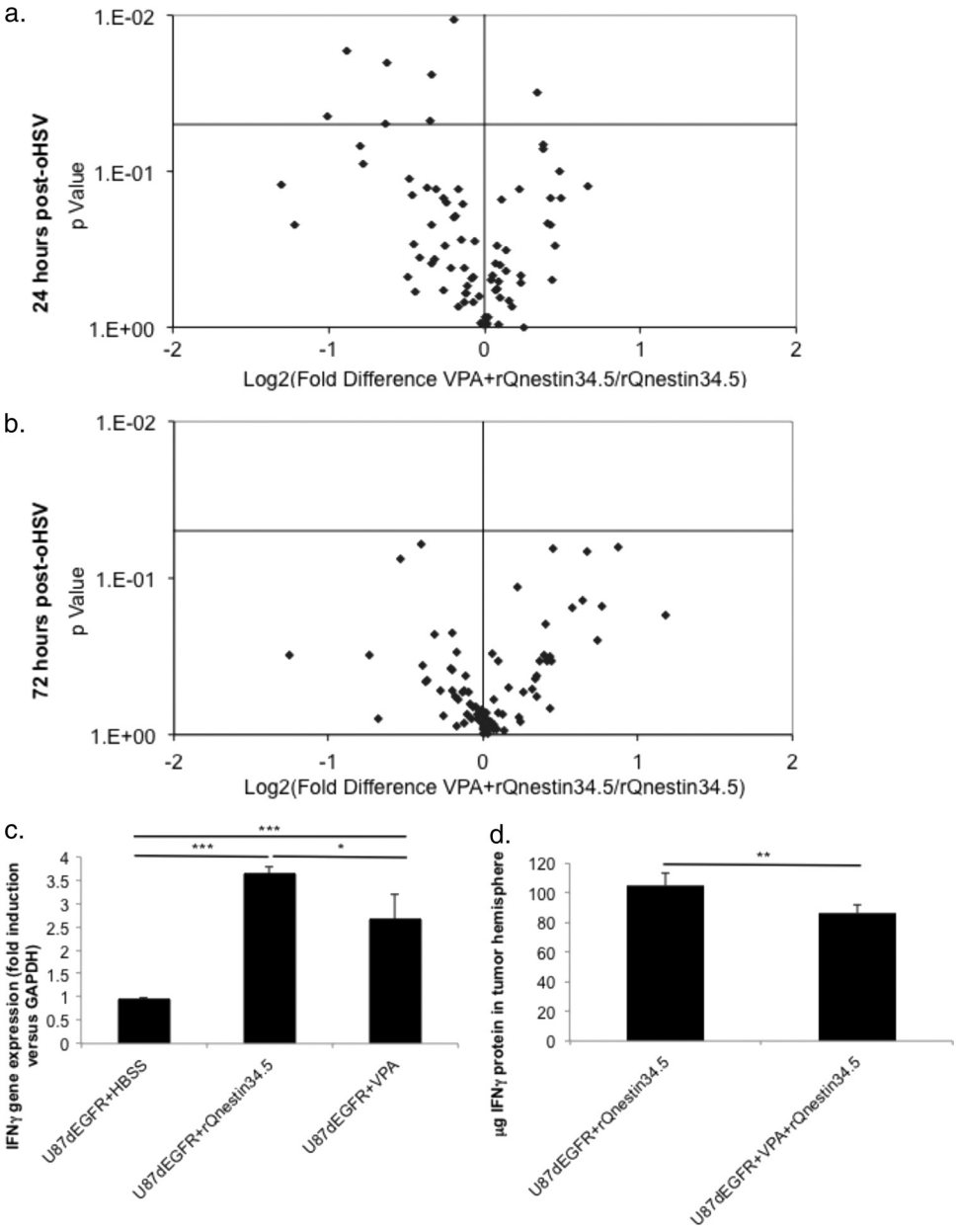

FIG 2 VPA cotherapy attenuates the inflammatory transcriptome following oHSV therapy. (a and b) Human U87dEGFR cells (10^5) were implanted intracranially into athymic mice brains and allowed to grow for 9 days. rQNestin34.5 (10^4 PFU/3 μl vehicle) was then stereotactically inoculated, using the same coordinates. For VPA-treated mice, two VPA treatments were performed at 12-h intervals the day before oHSV inoculation. At 24 (a) or 72 (b) h later, mice were sacrificed for mRNA isolation of the tumor-bearing hemisphere. Following mRNA conversion to cDNA, the expression of 84 mouse inflammatory genes was analyzed by quantitative RT-PCR and presented as a volcano plot of VPA-induced changes in expression of each inflammatory cytokine and receptor. This plot arranges genes along dimensions of biologic and statistical significance. The *x* axis indicates the $\log_2$ fold difference in gene expression for tumor tissue treated with VPA plus oHSV versus oHSV alone, and the *y* axis indicates *P* values obtained from the gene-specific *t* test on a negative log scale. The vertical line indicates no change relative to the control. The horizontal line indicates the threshold for a *P* value of 0.05 for the *t* test. Each point represents the mean value of the change in expression of an individual chemokine or chemokine receptor gene in tumors treated with VPA plus oHSV relative to tumors treated with oHSV alone. (c and d) Athymic mice were implanted with tumor, treated with VPA, and inoculated with rQNestin34.5 as described for panel a. Mice were sacrificed 24 h later for mRNA isolation and then cDNA synthesis or for protein extraction of the tumor-bearing hemisphere. The expression of IFN-γ was evaluated by real-time PCR (c) or ELISA (d), and two-sample *t* tests with Bonferroni adjustments were used to compare fold differences in expression levels. *, $P < 0.05$; **, $P < 0.01$; ***, $P < 0.001$. Error bars represent ± standard deviation.

first infected with oHSV (Fig. 5a). When NK cells were initially cultured overnight with 5.0 mM VPA, NK cell-mediated killing was significantly suppressed (Fig. 5a). Previous reports have demonstrated that treatment of various tumor target cells with HDACi, including VPA, increases their susceptibility to NK cell-mediated killing (6, 12, 51, 61). However, this has not been thoroughly investigated in glioblastomas. Therefore, we investigated whether VPA exposure to glioblastoma cells prior to coculture

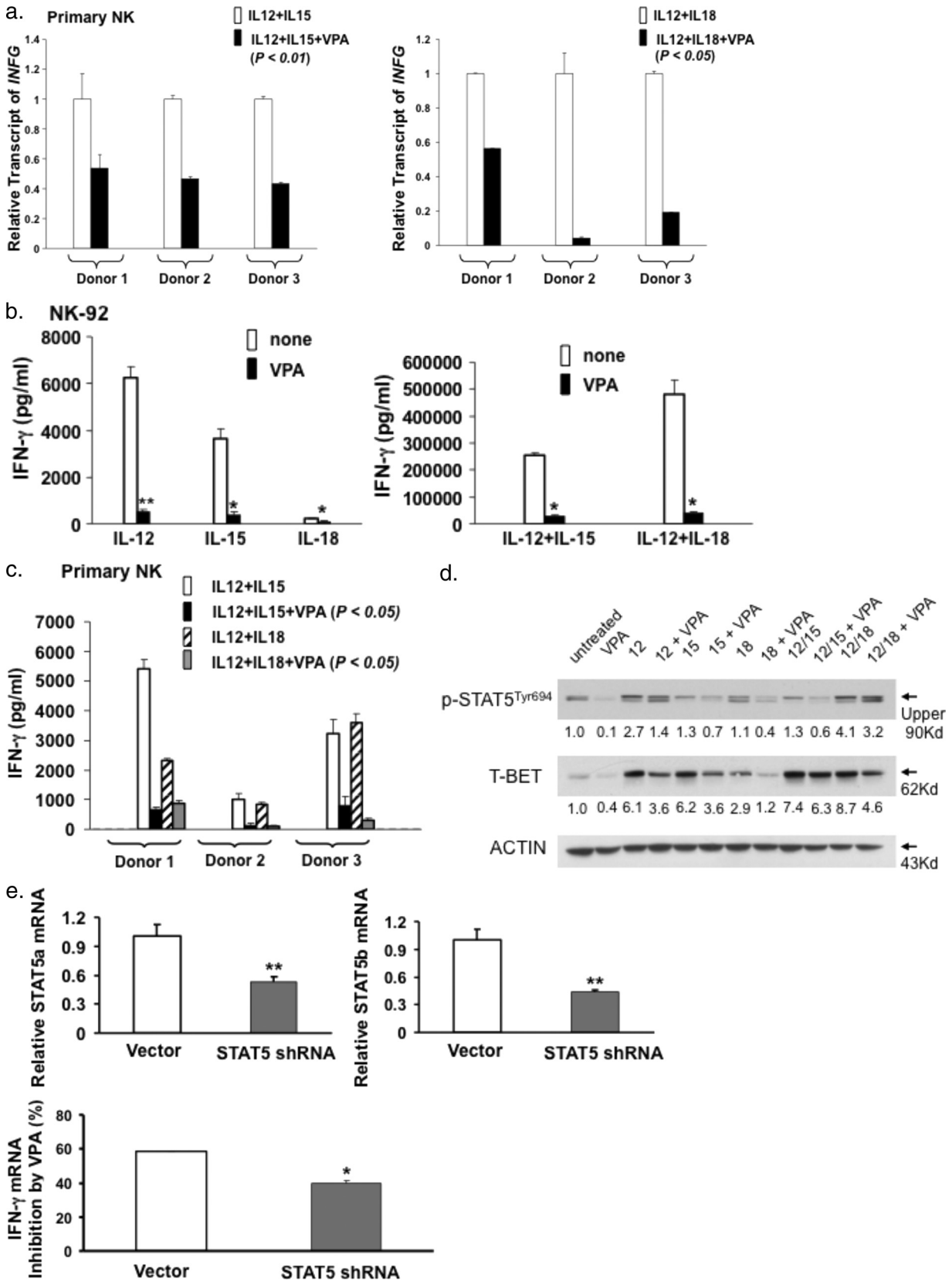

FIG 3 VPA suppression of IFN-γ production is associated with STAT5/T-BET inhibition. (a) Enriched human NK cells were cultured overnight with IL-12 plus IL-15 or IL-12 plus IL-18 in the presence or absence of VPA. The following day, NK cells were collected and mRNA was isolated. Following mRNA conversion to cDNA, the expression of IFN-γ was evaluated. Statistically significant values for VPA inhibition of IFN-γ transcript in primary NK cells costimulated with

with effector cells would alter the killing capacity of NK cells. In contrast to previous reports (6, 12, 51, 61), we found that pretreating U251 or Gli36dEGFR cells with VPA had no impact on the ability of NK cells to kill these targets (Fig. 5b). Moreover, when both NK and glioblastoma cells were treated overnight with or without VPA prior to coculture, glioblastoma lysis was still suppressed by VPA (Fig. 5b). Finally, we confirmed the applicability of these results to the NK response to wild-type HSV infection. While infection of U251 or Gli36dEGFR cells with wild-type HSV led to enhanced NK cell-mediated killing, VPA abrogated this response (Fig. 5c).

Since VPA is an FDA-approved agent for the treatment of epilepsy, we were interested to investigate whether its immunomodulatory effects would exacerbate HSV encephalitis. Although VPA treatment suppresses NK cell-mediated killing of virally infected normal human astrocytes (Fig. 5d), mice subjected to VPA cotreatment with wild-type HSV did not show significantly enhanced encephalitis compared to untreated mice infected with 10^3 (Fig. 5e) or 10^4 (see Fig. S3 in the supplemental material) wild-type HSV.

DISCUSSION

Combining oncolytic viruses with pharmacological modulators has proven in preclinical models to be a promising method for improving OV therapy. However, mechanisms of synergy have required additional studies. In our and other previous studies, VPA and other HDACi were shown to enhance OV replication through downregulation of type I IFN responses (33, 41, 42, 46). We hypothesized that this may lead to additional downregulation of antiviral innate cell responses. In this report, we demonstrate that VPA functions beyond inhibiting the virus-induced type I IFN response. As shown using a glioblastoma xenograft model, VPA combined with oHSV resulted in decreased immune cell activation at early time points after infection. Additionally, VPA potently suppressed NK cell-mediated cytotoxicity against virally infected glioblastoma cells and IFN-γ production and this was linked to suppression of STAT5 activity and T-BET expression. Despite this immunosuppressive profile, VPA treatment did not increase the susceptibility of HSV-treated mice to encephalitis. These findings suggest that while the mechanism of VPA's synergy with oHSV is multifaceted, it is mediated in part through the suppression of NK cells, which have been linked to a detrimental antiviral response to oHSV (17). Therefore, VPA exhibits pleiotropic mechanisms of action to enhance viral oncolysis by suppressing both intracellular and innate cellular antiviral responses.

As agents such as VPA gradually move toward testing in clinical trials, it is important to gain a greater appreciation for their mechanism of action. For instance, CPA has been shown to enhance OV efficacy not only through circumventing complement-mediated viral depletion but also through the attenuation of the antiviral response mediated by early immune responders (17, 25). CPA is currently being utilized as an adjuvant in cancer virotherapeutics trials utilizing measles virus (http://clinicaltrials.gov/ [NCT00450814]), reovirus (http://clinicaltrials.gov/ [NCT01240538]), and adenovirus (A. Hemminki, personal communication).

VPA, an FDA-approved agent for the treatment of epilepsy, has been recently described by members of our laboratory as an effective adjuvant for treatment of oHSV (46). Consequently, its multiple mechanisms of action are an area of interest. Apart from its anticancer properties, treatment combining VPA and oHSV achieved success through VPA's inhibition of expression of IFN-β and of the IFN-mediated proteins STAT1, PKR, and PML in infected cells (46). Trichostatin A (TSA), a similar HDACi, has also been paired with oHSV to increase oncolysis. In the context of TSA, therapeutic efficacy was achieved through inhibition of cyclin D1 and its concomitant arrest in cell cycle progression (3, 23, 30). Antitumor efficacy has also been achieved by an increase in TSA-mediated mitochondrial depolymerization and cleavage of caspases 3 and 9 when paired with oncolytic vesicular stomatitis virus (VSV) (41). Collectively, these findings demonstrate that HDAC inhibition facilitates successful OV therapy through various mechanisms within infected cells. However, the pleiotropic nature of these agents has not been studied in the context of the immune cell response to OV infection.

Our novel findings focus on VPA-mediated suppression of immune cell recruitment and activation following oHSV infection. Additionally, we have studied the ability of VPA to suppress NK cell activation and cytotoxicity in an *in vitro* model. The *in vivo* effect of VPA demonstrates that the recruitment of innate immune cells and the elaboration of inflammatory cytokines is suppressed initially after infection, thereby creating an environment that is more conducive to initial viral replication (17). Interestingly, the magnitude of this response is shorter in nature than what is seen with CPA cotherapy. As result, VPA could provide an important alternative cotherapy for oHSV treatment. One particular concern would be that VPA exposure could enhance susceptibility to wild-type HSV infection and concomitant toxicity. However, VPA combined with wild-type HSV did not result in significantly enhanced susceptibility to HSV encephalitis, suggesting that enhanced replication of oHSV in the presence of VPA is not applicable to WT HSV infection and/or that the short-term nature (within 72 h) of VPA's immunosuppressive effects was not deleterious to normal cells. Additional studies are needed to elucidate the relevance of these findings in comparisons of CPA and VPA cotherapy in the clinical setting. In

IL-12 and IL-15 or IL-12 and IL-18 were $P < 0.01$ for IL-12 and IL-15 costimulation and $P < 0.05$ for IL-12 and IL-18 costimulation. *P* values were calculated using Student's *t* test. (b) NK cell line NK-92 was cultured overnight with various combinations of cytokine stimulants in the presence or absence of VPA. The following day, secreted IFN-γ was quantified using ELISA. *P* values were calculated using Student's *t* test. (c) Enriched human NK cells from three separate donors were cultured overnight with various combinations of cytokine stimulants in the presence or absence of VPA. The following day, secreted IFN-γ was quantified using ELISA. A statistically significant value for VPA inhibition of IFN-γ protein secretion by primary NK cells costimulated with IL-12 and IL-15 or IL-12 and IL-18 was $P < 0.05$. *P* values were calculated using Student's *t* test. (d) Enriched primary human NK cells were cultured overnight with various combinations of cytokine stimulants in the presence or absence of VPA. The following day, extracted protein was evaluated by Western blotting for STAT5 phosphorylation (90 kDa [upper band]) or T-BET expression (62-kDa band). Actin was used as a loading control. Staining intensity was quantified with densitometry, and values are presented under the respective bands. (e) STAT5 knockdown was confirmed by real-time RT-PCR using NK-92 cells expressing STAT5-shRNA compared to the cells expressing the empty vector control (STAT5a, top left; STAT5b, top right). The STAT5-shRNA knockdown cell line or NK-92 cells expressing the empty vector control were used to determine IFN-γ inhibition by VPA in the presence of costimulation with IL-12 and IL-18 (bottom). *P* values were calculated using Student's *t* test. *, $P < 0.05$; **, $P < 0.01$. Error bars represent $\pm$ standard deviations.

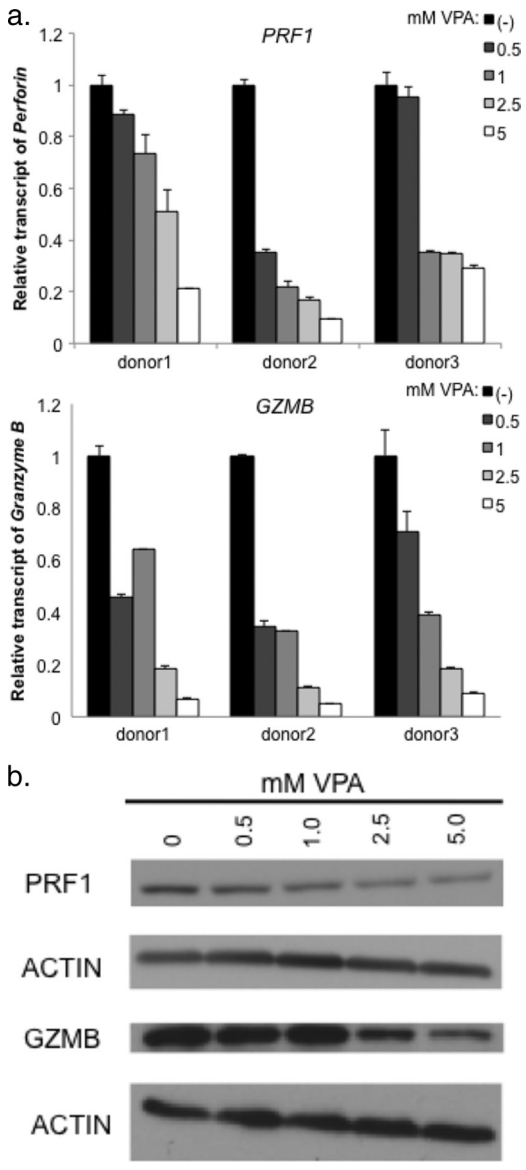

FIG 4 Mediators of NK cell cytotoxicity are reduced by VPA. (a) Enriched human NK cells were cultured overnight in the absence or presence of increasing amounts of VPA. The following day, NK cells were collected and mRNA was isolated. Following mRNA conversion to cDNA, expression of perforin (PRF1) and granzyme B (GZMB) was evaluated. A statistically significant value for VPA inhibition of perforin transcript at a concentration of 2.5 μM was $P < 0.05$ and at 5 μM was $P < 0.01$. A statistically significant value for VPA inhibition of granzyme B transcript at a concentration of 0.5 μM was $P < 0.05$, at 1 μM was $P < 0.05$, at 2.5 μM was $P < 0.001$, and at 5 μM was $P < 0.001$. P values were calculated using Student's t test. (b) Enriched human NK cells were treated as described for panel a. The following day, extracted protein was evaluated using Western blot analysis of perforin and granzyme B expression. Actin was used as a loading control. Error bars represent ± standard deviations.

particular, attention should be given to differences in dosing regimens, toxicity-associated immunosuppression, and the ability to bypass initial antiviral mediators while eliciting downstream antitumor immunity.

Our *in vitro* findings suggest that VPA significantly suppressed NK cell production of IFN-γ at least in part via a STAT5/T-BET-dependent mechanism. In support of this, we found that VPA suppresses STAT5 phosphorylation and T-BET expression. Moreover, STAT5-shRNA reduced the capacity for IFN-γ inhibition by VPA in NK-92 cells, although our efforts to establish a T-BET knockdown NK cell line were unsuccessful. Interestingly, VPA strongly inhibited IFN-γ production, but the magnitude of this effect was not as strong for P-STAT5 and T-BET (compare Fig. 3d with 3a to c). Biologically, this might be explained by a small change in an effector molecule (STAT-5/T-BET) amplified severalfold downstream (IFN-γ). It might also have been due to STAT5/T-BET-independent pathways that mediate inhibition of IFN-γ by VPA. A possible technical explanation is that it was due to the inability to precisely correlate a quantitative ELISA result with a semiquantitative Western blot analysis result. Further experiments are required to explain this.

Our results show that expression of several NK cell cytotoxic markers and receptors (such as NKp46) was reduced by VPA (see Table S1 in the supplemental material). Ogbomo et al. also showed that pretreatment of NK cells with the HDACi suberoylanilide hydroxamic acid or valproic acid significantly inhibited NK cell cytotoxicity against human leukemic cells (44). This was associated with reduced NKp30 and NKp46 natural cytotoxicity receptor expression, impaired granule exocytosis, and inhibition of NF-κB (44). However, in contrast to our findings and the work of Ogbomo et al. showing that VPA suppresses NK cytotoxic activity, several groups have reported that HDACi can enhance NK cell-mediated killing through increased NK ligand expression on tumor cells. Zhang et al. have reported that enhanced susceptibility to NK cell-mediated killing occurs following sodium butyrate treatment of HeLA and HepG2 tumor cell lines due to enhanced expression of the NKG2D ligands major histocompatibility complex (MHC) class I-related chain molecules A and B (MICA and MICB) (61). Skov et al. similarly found that HDAC inhibition led to increases in both expression of MICA and MICB on a variety of tumors cells and subsequent NK cell-mediated killing (51). Finally, Armeanu et al. detected increased expression of MICA and MICB in hepatocellular carcinoma cells treated with VPA, rendering the cells more susceptible to NK cell-mediated lysis (6). In summary, note that all these studies focused on the ability of HDACi to modify target cells instead of NK cells.

To understand these differences, it may be essential to differentiate between the effects of HDACi on NK versus target cells. Unlike previous studies that demonstrated increased NK killing following target cell, but not NK cell, exposure to HDACi, our report is the first to show that treatment of NK cells with VPA results in reduced NK cell-mediated killing regardless of the presence or absence of VPA exposure to the glioblastoma target cells. These findings suggest that when both NK cells and target cells are exposed to HDACi, the reduction in target cell lysis may be explained by the decreased cytotoxic potential of treated NK cells despite the presence of NK ligands on the surface of treated target cells. While these findings do not argue against the use of VPA to induce enhanced NK cell-mediated killing, they do call for caution when designing immunotherapy and adoptive therapy trials to ensure that the HDACi-induced increase in NK ligand expression is not counteracted by suppression of NK cell cytotoxicity.

As oncolytic viral cotherapies with pharmacological agents are increasingly pursued for implementation in the clinic, it is essen-

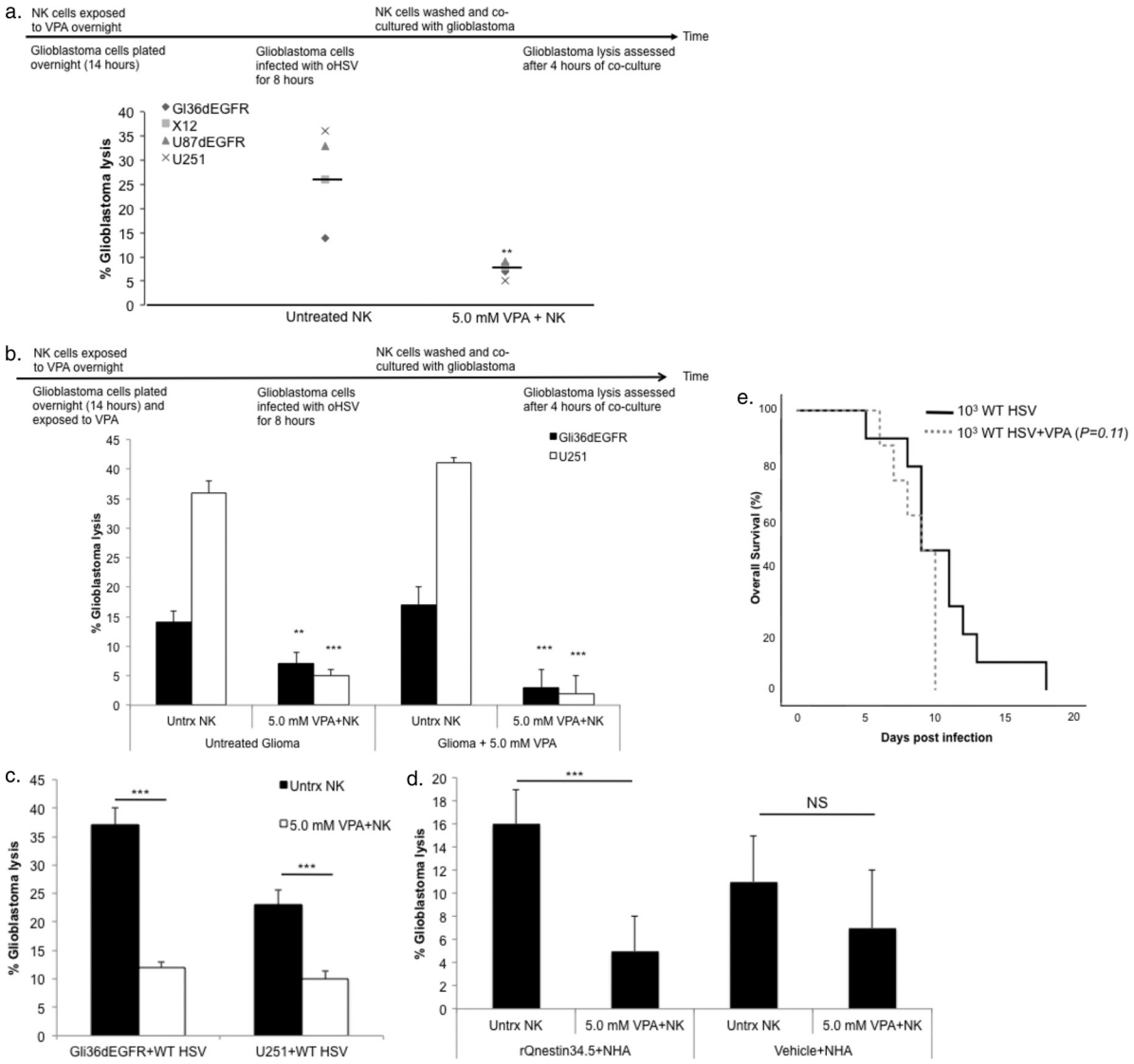

FIG 5 NK cell-mediated killing of oHSV-infected glioblastoma cells is suppressed by VPA. (a) Enriched human NK cells were exposed to 5.0 mM VPA overnight. Gli36dEGFR, U87dEGFR, and U251 glioblastoma cell lines and X12 "stem-like" glioblastoma cells were plated (10^4 cells/well); 14 h later, glioblastoma cells were washed and infected with rQNestin34.5 (MOI of 1.0) for 8 h prior to coculture with NK cells. VPA-treated NK cells were washed and cocultured with infected glioblastoma cells at an effector/target ratio of 12:1 in the presence of IL-15 (100 ng/ml), added immediately before coculture with infected cells. At 4 h later, glioblastoma lysis was assessed. The percentage of glioblastoma lysis for each cell type is plotted for NK cells with or without VPA. Horizontal bars indicate the mean values for individual events. (b) Enriched human NK cells were exposed to 5.0 mM VPA overnight. Gli36dEGFR or U251 cells were plated (10^4 cells/well) and were either left untreated (Untrx) or exposed to 5.0 mM VPA overnight. At 14 h later, glioblastoma cells were washed and infected with rQNestin34.5 (MOI of 1.0) for 8 h prior to coculture with NK cells. VPA-treated NK cells were washed and then cocultured as described for panel a. (c) Gli36dEGFR and U251 cells were plated (10^4 cells/well) and infected with wild-type HSV (MOI of 1.0) for 8 h. Enriched human NK cells were treated with VPA, washed, and cocultured with infected glioblastoma as described for panel a. (d) Normal human astrocytes were plated (10^4 cells/well) and infected with rQNestin34.5 (MOI of 1.0) or mock infected for 8 h. Enriched human NK cells were treated with VPA, washed, and cocultured with infected glioblastoma as described for panel a. (e) Glioblastoma-free athymic mice were either treated with vehicle or subjected to two VPA treatments at 12-h intervals the day before wild-type HSV inoculation. The following day, wild-type HSV (10^3 PFU) was inoculated intracranially and mice were monitored for the onset of neurological symptoms. For panels a to d, a *t* test was used to compare percentages of glioblastoma lysis in the presence or absence of VPA. For panel e, a log-rank test was used to compare animal survival rates. **, $P < 0.01$; ***, $P < 0.001$. Error bars represent ± standard deviations.

tial to understand the mechanisms through which efficacy is being achieved. In this study, VPA coadministration was shown to attenuate the elicited host immune response to oncolytic virus. This mechanism of action is in addition to the previously uncovered mechanism of circumventing host cell antiviral defenses (46). In addition, we have uncovered a novel mechanism by which VPA suppresses human NK cell cytotoxicity and IFN-γ production. Taken together, these findings provide insights that can be used to enhance subsequent studies that attempt to target HDAC inhibition and suppress NK cell activity.

ACKNOWLEDGMENTS

This work was supported by NIH grants 7U01NS061811 (to E.A.C.), CA069246 (to E.A.C.), CA68458 (to M.A.C.), and CA98472 (to M.A.C.),

and TL1RR025753 (to C.A.A.-B.). C.A.A.-B. was supported by an American Medical Association Foundation Seed Grant. This work was also supported by the Dardinger Neuro-oncology Laboratory.

REFERENCES

1. **Aghi M, Visted T, Depinho RA, Chiocca EA.** 2008. Oncolytic herpes virus with defective ICP6 specifically replicates in quiescent cells with homozygous genetic mutations in p16. Oncogene **27**:4249–4254.
2. **Ahmed AU, et al.** 2010. Bone marrow mesenchymal stem cells loaded with an oncolytic adenovirus suppress the anti-adenoviral immune response in the cotton rat model. Mol. Ther. **18**:1846–1856.
3. **Alao JP.** 2007. The regulation of cyclin D1 degradation: roles in cancer development and the potential for therapeutic invention. Mol. Cancer **6**:24.
4. **Altomonte J, et al.** 2008. Exponential enhancement of oncolytic vesicular stomatitis virus potency by vector-mediated suppression of inflammatory responses in vivo. Mol. Ther. **16**:146–153.
5. **Alvarez-Breckenridge C, Kaur B, Chiocca EA.** 2009. Pharmacologic and chemical adjuvants in tumor virotherapy. Chem. Rev. **109**:3125–3140.
6. **Armeanu S, et al.** 2005. Natural killer cell-mediated lysis of hepatoma cells via specific induction of NKG2D ligands by the histone deacetylase inhibitor sodium valproate. Cancer Res. **65**:6321–6329.
7. **Chang HM, et al.** 2004. Induction of interferon-stimulated gene expression and antiviral responses require protein deacetylase activity. Proc. Natl. Acad. Sci. U. S. A. **101**:9578–9583.
8. **Chen S, Kawashima H, Lowe JB, Lanier LL, Fukuda M.** 2005. Suppression of tumor formation in lymph nodes by L-selectin-mediated natural killer cell recruitment. J. Exp. Med. **202**:1679–1689.
9. **Chen WY, Bailey EC, McCune SL, Dong JY, Townes TM.** 1997. Reactivation of silenced, virally transduced genes by inhibitors of histone deacetylase. Proc. Natl. Acad. Sci. U. S. A. **94**:5798–5803.
10. **Chiocca EA.** 2002. Oncolytic viruses. Nat. Rev. Cancer **2**:938–950.
11. **Chiocca EA, et al.** 2004. A phase I open-label, dose-escalation, multi-institutional trial of injection with an E1B-attenuated adenovirus, ONYX-015, into the peritumoral region of recurrent malignant gliomas, in the adjuvant setting. Mol. Ther. **10**:958–966.
12. **Diermayr S, et al.** 2008. NKG2D ligand expression in AML increases in response to HDAC inhibitor valproic acid and contributes to allorecognition by NK-cell lines with single KIR-HLA class I specificities. Blood **111**:1428–1436.
13. **Dion LD, et al.** 1997. Amplification of recombinant adenoviral transgene products occurs by inhibition of histone deacetylase. Virology **231**:201–209.
14. **Forsyth P, et al.** 2008. A phase I trial of intratumoral administration of reovirus in patients with histologically confirmed recurrent malignant gliomas. Mol. Ther. **16**:627–632.
15. **Fouladi M.** 2006. Histone deacetylase inhibitors in cancer therapy. Cancer Invest. **24**:521–527.
16. **Freeman AI, et al.** 2006. Phase I/II trial of intravenous NDV-HUJ oncolytic virus in recurrent glioblastoma multiforme. Mol. Ther. **13**:221–228.
17. **Fulci G, et al.** 2006. Cyclophosphamide enhances glioma virotherapy by inhibiting innate immune responses. Proc. Natl. Acad. Sci. U. S. A. **103**:12873–12878.
18. **Fulci G, et al.** 2007. Depletion of peripheral macrophages and brain microglia increases brain tumor titers of oncolytic viruses. Cancer Res. **67**:9398–9406.
19. **Fuller CL, et al.** 2007. NKp30-dependent cytolysis of filovirus-infected human dendritic cells. Cell Microbiol. **9**:962–976.
20. **Génin P, Morin P, Civas A.** 2003. Impairment of interferon-induced IRF-7 gene expression due to inhibition of ISGF3 formation by trichostatin A. J. Virol. **77**:7113–7119.
21. **Giannini C, et al.** 2005. Patient tumor EGFR and PDGFRA gene amplifications retained in an invasive intracranial xenograft model of glioblastoma multiforme. Neuro. Oncol. **7**:164–176.
22. **Harrow S, et al.** 2004. HSV1716 injection into the brain adjacent to tumour following surgical resection of high-grade glioma: safety data and long-term survival. Gene Ther. **11**:1648–1658.
23. **Hu J, Colburn NH.** 2005. Histone deacetylase inhibition down-regulates cyclin D1 transcription by inhibiting nuclear factor-kappaB/p65 DNA binding. Mol. Cancer Res. **3**:100–109.
24. **Iankov I, Hillestad M, Dietz A, Russell S, Galanis E.** 2009. Converting tumor-specific markers into reporters of oncolytic virus infection. Mol. Ther. **17**:1395–1403.
25. **Ikeda K, et al.** 1999. Oncolytic virus therapy of multiple tumors in the brain requires suppression of innate and elicited antiviral responses. Nat. Med. **5**:881–887.
26. **Ikeda K, et al.** 2000. Complement depletion facilitates the infection of multiple brain tumors by an intravascular, replication-conditional herpes simplex virus mutant. J. Virol. **74**:4765–4775.
27. **Kambara H, Okano H, Chiocca EA, Saeki Y.** 2005. An oncolytic HSV-1 mutant expressing ICP34.5 under control of a nestin promoter increases survival of animals even when symptomatic from a brain tumor. Cancer Res. **65**:2832–2839.
28. **Kambara H, Saeki Y, Chiocca EA.** 2005. Cyclophosphamide allows for in vivo dose reduction of a potent oncolytic virus. Cancer Res. **65**:11255–11258.
29. **Kircher B, et al.** 2009. Anti-leukemic activity of valproic acid and imatinib mesylate on human Ph+ ALL and CML cells in vitro. Eur. J. Haematol. **83**:48–56.
30. **Knudsen KE, Diehl JA, Haiman CA, Knudsen ES.** 2006. Cyclin D1: polymorphism, aberrant splicing and cancer risk. Oncogene **25**:1620–1628.
31. **Kurozumi K, et al.** 2008. Oncolytic HSV-1 infection of tumors induces angiogenesis and upregulates CYR61. Mol. Ther. **16**:1382–1391.
32. **Li H, Zeng Z, Fu X, Zhang X.** 2007. Coadministration of a herpes simplex virus-2 based oncolytic virus and cyclophosphamide produces a synergistic antitumor effect and enhances tumor-specific immune responses. Cancer Res. **67**:7850–7855.
33. **Liu T-C, Castelo-Branco P, Rabkin SD, Martuza RL.** 2008. Trichostatin A and oncolytic HSV combination therapy shows enhanced antitumoral and antiangiogenic effects. Mol. Ther. **16**:1041–1047.
34. **Lun XQ, et al.** 2009. Efficacy of systemically administered oncolytic vaccinia virotherapy for malignant gliomas is enhanced by combination therapy with rapamycin or cyclophosphamide. Clin. Cancer Res. **15**:2777–2788.
35. **Markert JM, et al.** 2009. Phase Ib trial of mutant herpes simplex virus G207 inoculated pre- and post-tumor resection for recurrent GBM. Mol. Ther. **17**:199–207.
36. **Markert JM, et al.** 2000. Conditionally replicating herpes simplex virus mutant, G207 for the treatment of malignant glioma: results of a phase I trial. Gene Ther. **7**:867–874.
37. **Marks P, et al.** 2001. Histone deacetylases and cancer: causes and therapies. Nat. Rev. Cancer **1**:194–202.
38. **Marques CP, et al.** 2008. Prolonged microglial cell activation and lymphocyte infiltration following experimental herpes encephalitis. J. Immunol. **181**:6417–6426.
39. **Moretta A, et al.** 1991. CD69-mediated pathway of lymphocyte activation: anti-CD69 monoclonal antibodies trigger the cytolytic activity of different lymphoid effector cells with the exception of cytolytic T lymphocytes expressing T cell receptor alpha/beta. J. Exp. Med. **174**:1393–1398.
40. **Myers RM, et al.** 2007. Preclinical pharmacology and toxicology of intravenous MV-NIS, an oncolytic measles virus administered with or without cyclophosphamide. Clin. Pharmacol. Ther. **82**:700–710.
41. **Nguyên TL, et al.** 2008. Chemical targeting of the innate antiviral response by histone deacetylase inhibitors renders refractory cancers sensitive to viral oncolysis. Proc. Natl. Acad. Sci. U. S. A. **105**:14981–14986.
42. **Nguyen TL-A, Wilson MG, Hiscott J.** 2010. Oncolytic viruses and histone deacetylase inhibitors—a multi-pronged strategy to target tumor cells. Cytokine Growth Factor Rev. **21**:153–159.
43. **Nusinzon I, Horvath CM.** 2006. Positive and negative regulation of the innate antiviral response and beta interferon gene expression by deacetylation. Mol. Cell. Biol. **26**:3106–3113.
44. **Ogbomo H, Michaelis M, Kreuter J, Doerr HW, Cinatl J.** 2007. Histone deacetylase inhibitors suppress natural killer cell cytolytic activity. FEBS Lett. **581**:1317–1322.
45. **Ostertag D, et al.** 2011. Brain tumor eradication and prolonged survival from intratumoral conversion of 5-fluorocytosine to 5-fluorouracil using a nonlytic retroviral replicating vector. Neuro. Oncol. **14**:145–159.
46. **Otsuki A, et al.** 2008. Histone deacetylase inhibitors augment antitumor efficacy of herpes-based oncolytic viruses. Mol. Ther. **16**:1546–1555.
47. **Papanastassiou V, et al.** 2002. The potential for efficacy of the modified (ICP 34.5(-)) herpes simplex virus HSV1716 following intratumoural injection into human malignant glioma: a proof of principle study. Gene Ther. **9**:398–406.

48. **Park IK, et al.** 2009. The Axl/Gas6 pathway is required for optimal cytokine signaling during human natural killer cell development. Blood **113**: 2470–2477.
49. **Qiao J, et al.** 2008. Cyclophosphamide facilitates antitumor efficacy against subcutaneous tumors following intravenous delivery of reovirus. Clin. Cancer Res. **14**:259–269.
50. **Rampling R, et al.** 2000. Toxicity evaluation of replication-competent herpes simplex virus (ICP 34.5 null mutant 1716) in patients with recurrent malignant glioma. Gene Ther. **7**:859–866.
51. **Skov S, et al.** 2005. Cancer cells become susceptible to natural killer cell killing after exposure to histone deacetylase inhibitors due to glycogen synthase kinase-3-dependent expression of MHC class I-related chain A and B. Cancer Res. **65**:11136–11145.
52. **Smith KM, Wu J, Bakker AB, Phillips JH, Lanier LL.** 1998. Ly-49D and Ly-49H associate with mouse DAP12 and form activating receptors. J. Immunol. **161**:7–10.
53. **Tang X, et al.** 2007. Acetylation-dependent signal transduction for type I interferon receptor. Cell **131**:93–105.
54. **Thorne SH, et al.** 2010. Targeting localized immune suppression within the tumor through repeat cycles of immune cell-oncolytic virus combination therapy. Mol. Ther. **18**:1698–1705.
55. **Trotta R, Ciarlariello D, Dal Col J, Allard J II, et al.** 2007. The PP2A inhibitor SET regulates natural killer cell IFN-gamma production. J. Exp. Med. **204**:2397–2405.
56. **Wakimoto H, Fulci G, Tyminski E, Chiocca EA.** 2004. Altered expression of antiviral cytokine mRNAs associated with cyclophosphamide's enhancement of viral oncolysis. Gene Ther. **11**:214–223.
57. **Walzer T, et al.** 2007. Identification, activation, and selective in vivo ablation of mouse NK cells via NKp46. Proc. Natl. Acad. Sci. U. S. A. **104**:3384–3389.
58. **Walzer T, Dalod M, Vivier E, Zitvogel L.** 2005. Natural killer cell-dendritic cell crosstalk in the initiation of immune responses. Expert Opin. Biol. Ther. **5**(Suppl. 1):S49–S59.
59. **Yamano T, et al.** 2000. Amplification of transgene expression in vitro and in vivo using a novel inhibitor of histone deacetylase. Mol. Ther. **1**:574–580.
60. **Yu J, et al.** 2006. Pro- and antiinflammatory cytokine signaling: reciprocal antagonism regulates interferon-gamma production by human natural killer cells. Immunity **24**:575–590.
61. **Zhang C, Wang Y, Zhou Z, Zhang J, Tian Z.** 2009. Sodium butyrate upregulates expression of NKG2D ligand MICA/B in HeLa and HepG2 cell lines and increases their susceptibility to NK lysis. Cancer Immunol. Immunother. **58**:1275–1285.